

## An in-process, layer wise surface metrology system for a new E-Beam additive manufacturing machine

Liam Blunt<sup>1</sup>\*Yue Liu<sup>1</sup>, Zonghua Zhang<sup>2</sup>, Chris Smith<sup>3</sup> David Knight<sup>3</sup>, Feng Gao<sup>1</sup>, Andrew Townsend<sup>1</sup> Xiangqian Jiang<sup>1</sup>

1. EPSRC Future Metrology Hub, University of Huddersfield UK.

2. School of Mechanical Engineering, Hebei University of Technology, Tianjin, China. 3. Wayland Additive, UK.

[l.a.blunt@hud.ac.uk](mailto:l.a.blunt@hud.ac.uk)

### Abstract

Additive manufacturing (AM) of metal powder by electron beam fusion offers significant advantages compared with traditional subtractive manufacturing techniques as well as certain advantages of production rate and post processing, over laser SLM systems. EBM AM technologies have continued to develop over recent years in particular for medical implants and aerospace parts, and new vendors of such AM machines are developing more advanced systems with additional in process metrology. In spite of the clear advantages, E beam AM suffers from limitations which need to be addressed before wider take up of the technology is achieved.

During the powder delivery process, which occurs many thousands of times during a part build, there is potential for defects in the powder delivery process. Such defects take the form of score trenches running perpendicular to the powder delivery direction, vibration ripples parallel to the delivery direction, excessive powder delivery due to damage to the powder rake and lack of powder due to under dosing problems. Like-wise during the layer build process it is important to monitor out of plane defects on parts such as thermal swelling. In-plane information regarding the boundary of the melted powder and unmelted powder are equally important to monitor in plane geometry.

This paper describes the development and deployment of a newly patented, in-process metrology system on a recently launched commercial EBM AM machine. The inspection system, which is fully integrated into the AM machine control system, is based on single camera, phase measurement profilometry. A temporal synchronisation technique is employed for data capture and using automatic machine triggering an acquisition time of 2 seconds per measurement is achieved. A novel calibration method based on a surface fitting algorithm is deployed to reduce the influence of phase error and random noise. The paper gives examples of the system being deployed on the build of typical parts and shows examples of powder delivery assessment and post build layer measurement and describes the integration of the metrology system with the AM machine control systems.

Electron beam, phase measurement profilometry, surface metrology, powder bed, out of plane error.

### 1. Introduction

The development and implementation of in-process, layer wise surface metrology technique has for some time been a research goal in AM<sup>1</sup>. A range of inspection systems have been embedded in AM tool for monitoring, such as infrared thermal inspection, photogrammetry and profilometry<sup>2</sup>. As well as layer wise part geometry, the powder delivery process, there is potential for defect generation which take the form of score trenches running perpendicular to the powder delivery direction, vibration ripples parallel to the delivery direction, excessive powder delivery due to damage to the powder rake and lack of powder due to under dosing problems. This paper describes the development and deployment of a newly patented, in-process metrology system which is based on single camera system using phase measurement profilometry. The metrology system is now deployed recently launched commercial E-Beam AM machine.

This paper gives a brief introduction to the embedded fringe projection inspection system hosted in the AM machine and outlines the measurement principle. A novel system calibration

method is introduced and examples of real measurements of the powder bed and part are demonstrated.

### 2. Methods

#### 2.1. Inspection system for AM

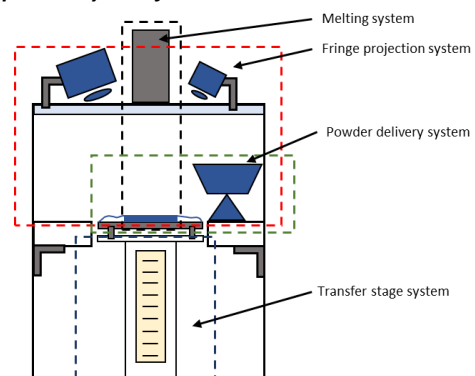


**Figure 1.** A conceptual set up of the detection system  
The newly development commercial EBM machine comprises an electron beam melting source, powder delivery system, a

powder bed transfer system and the fringe projection inspection set up, as shown in Figure 1. The inspection system is fixed on top of the machine outside of the vacuum chamber and the powder bed is “viewed” through leaded glass windows. The fringe projection system consists of a CCD (charge-coupled device) camera and a DLP (digital light processing) projector. During the manufacturing process as shown in Figure 2, after process parameters are set, a layer of powder is dispensed from a powder hopper. Then the fringe projection system inspects the powder bed to assess if the surface is defect free enough to proceed with the process. If the results are deemed “good”, the system will carry on with the build, namely powder fusion. Otherwise, the power delivery will be repeated until the surface is smooth enough or there is operator intervention. Following a layer of powder fusion, the fringe projection system will inspect the printed part to detect planar and out of plane error. If no problems are detected or the problem can be resolved the build will carry on, if a problem is detected (i.e. the part build deviation is beyond a given threshold) then the build is halted. This whole process is repeated throughout the build cycle until the build is complete. Between powder delivery and melting, there are 4 to 5 seconds preparation time, the fringe projection system make use of this interlude to inspect the powder bed and so will not increase the total build time. The fringe projection system can achieve in-process out-of-plane defects inspection, such as rake damage, delamination, swelling, porosity, lack of powder etc.

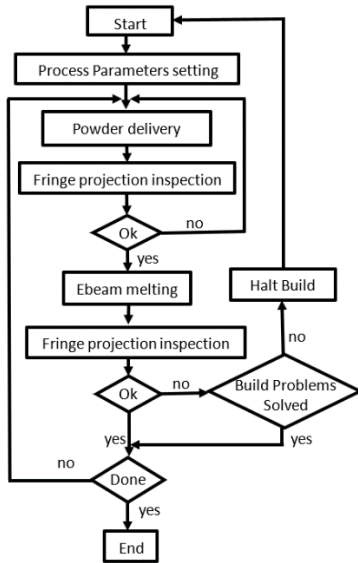


Figure 2. A flow chart of build process

## 2.2. Measurement principle

In order to obtain shape information, the geometric relationship of the DLP projector and the CCD camera should be determined. The sinusoidal fringe patterns are projected onto the test surface where, the fringe patterns are deformed due to surface perturbations, and the deformed fringes are captured by the camera. Phase information is computed from the captured deformed fringe patterns. After system calibration, 3D shape data can be obtained using the phase information.

A reference surface  $M$  is set as a datum plane to establish a reference coordinate system. The relationship between the absolute phase map and depth data can be established in the reference coordinate system as follows:

$$Z_r(x, y) = \sum_{n=0}^N a_n(x, y) \Delta\phi(x, y)^n \quad (1)$$

where  $a_n, a_{n-1}, a_2, a_1$  are sets of coefficients containing the system parameters,  $Z$  is the height value relative to reference plane  $M$ .  $\Delta\phi$  is the absolute unwrapped phase difference between the measured surface and the reference surface  $M$ . Therefore, the height values across the surface can be calculated with the phase information and system coefficients.

To obtain height values by using Equation 1, it is essential to analyze phase values accurately. In this paper, a phase shifting algorithm and an optimum frequency selection algorithm are used to obtain absolute phase information<sup>3</sup>. In the present case a wrapped phase can be represented by the following equation:

$$W(\phi) = -\arctan\left(\frac{\sum_{i=1}^N I_i(x, y) \sin(\delta_i)}{\sum_{i=1}^N I_i(x, y) \cos(\delta_i)}\right) \quad (2)$$

Where  $I_i$  is the captured fringe pattern intensity,  $\delta_i$  is phase shifting steps. After calculating the wrapped phase, the absolute phase data can be obtained by a temporal phase unwrapping method (optimum frequency selection algorithm). Sets of sequential sinusoidal fringe patterns are projected onto test surface and the number of fringes are defined by the following equation :

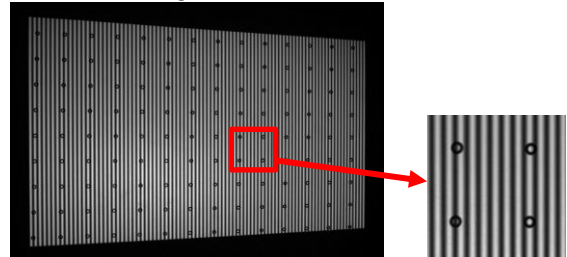
$$N_{fi} = N_{f0} - (N_{f0})^{\frac{(i-1)}{(m-1)}}, i = 1, 2, \dots, m - 1 \quad (3)$$

Where  $N_{f0}$  is the maximum number of fringes,  $N_{fi}$  is the number of fringes in the  $i^{\text{th}}$  fringe set, and  $m$  is the number of fringe sets used. In this paper, the maximum number of fringes is 100, and  $m=3$ , therefore  $N_{f1}=99$  and  $N_{f2}=90$ .

## 3. System calibration

In order to obtain an accurate 3D shape, a significant step for an optical system is to find the spatial relationship between the camera and the projector, known as 3D calibration, this effectively determines the measurement accuracy<sup>4</sup>. A white ceramic diffuse plate with certified concentric circles markings was employed as a calibration board during the system calibration. In this paper, based on a polynomial calibration technique, a novel surface fitting calibration method is reported to reduce random noise and eliminate the calibration induced “circle mark” effect.

The sets of sinusoidal fringes are projected onto the calibration board. Due to the presence of the black circle rings on the calibration board the rings absorb part of the light, the captured fringe patterns have low fringe contrast on the circle area, which results in phase error and measurement error, as demonstrated in Figure 3.



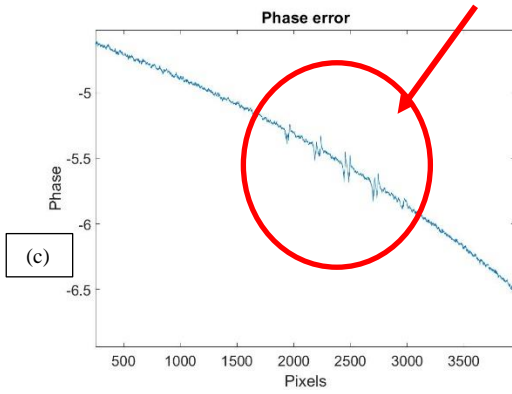


**Figure 3.** The impact of calibration board black circle rings on captured phase data

A novel calibration approach based on a curve fitting algorithm was applied to solve this problem. The noisy points were removed by calculating the modulation of the fringe patterns. The outliers crossing the circle ring area are then removed. The unwrapped phase map is calculated from the rest of the wrapped phase data by using the optimum 3-frequency selection algorithm<sup>5,6</sup>.

In order to fill in the invalid points, a quintic polynomial fitting equation was investigated to match the unwrapped phase data as follows:

$$FittingPhase = P_0 + P_1x + P_2y + P_3x^2 + P_4xy + P_5y^2 + P_6x^3 + P_7x^2y + P_8xy^2 + P_9y^3 + P_{10}x^4 + P_{11}x^3y + P_{12}x^2y^2 + P_{13}xy^3 + P_{14}y^4 + P_{15}x^5 + P_{16}x^4y + P_{17}x^3y^2 + P_{18}x^2y^3 + P_{19}xy^4 + P_{20}y^5 \quad (9)$$

where  $x$  and  $y$  are the pixels positions,  $P_n$  is the coefficients of the fitting equation. Because the calibration board is a flat white ceramic plate, the unwrapped phase map of the calibration board is ideally a plane. A relatively high order fitting (quantic polynomial fitting) can meet measurement requirements.

#### 4. Measurement

Following successful implementation of a prototype system, full implementation of the inspection system was carried out on a newly developed commercial EBM machine. The inspection system realised layer-wise inspection. Figure 4 shows a series of in-situ measurement results during a part build process. The images show results for a build where images from steps of 15 layers are shown for clarity. Figure 4 shows the measurement results after powder delivery of layers 45(a), 60(b), 75(c), 90(d), 105(e) and 120(f), respectively. The figures show two simple annular parts during a build process. It is clear from the figures that thermal swelling of the inner radius increases through the build cycle and in figures 4 (b) (c) and (e) show a wake effect in the powder delivery resulting from the swelling and a consequent powder delivery shadowing effect. A height threshold on captured images can be used to halt the build in the presence of significant part swelling. Note, such part swelling can eventually damage the powder delivery rake. The results show the fringe projection system has the capability to detect part thermal swelling, lack of powder delivery and other powder bed defects/effects for this build.

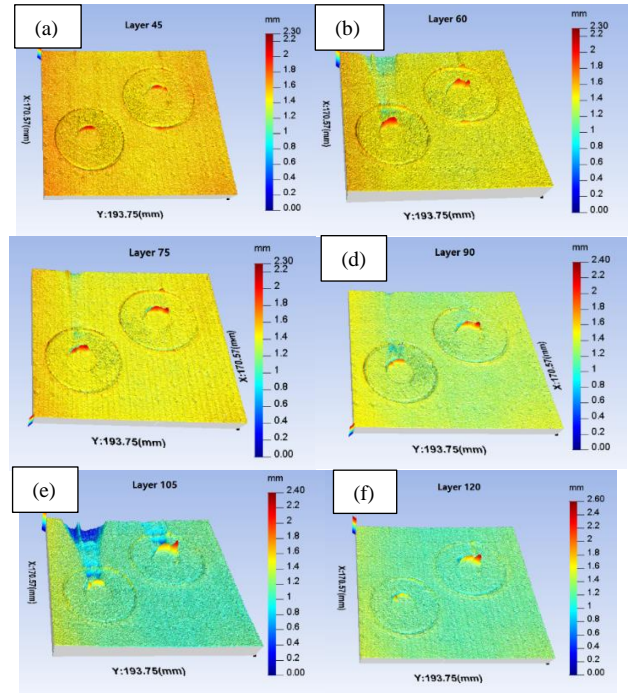
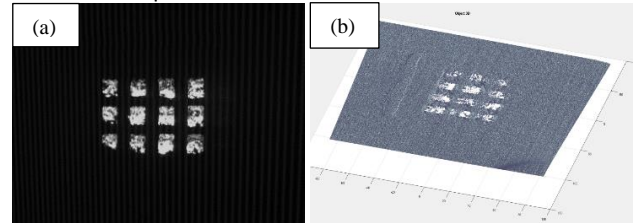


**Figure 4.** 3D measurement results of the building process (powder deliver direction from front to back of image)

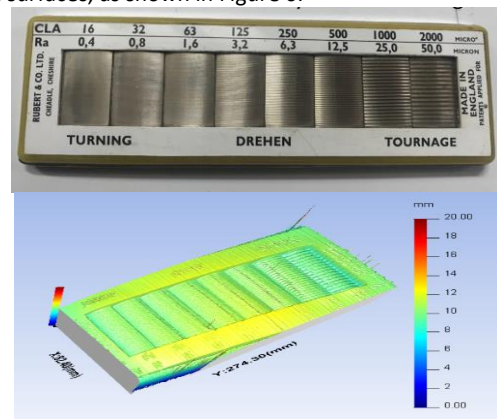
During manufacturing procedure, after the powder melting, the fringe projection system will inspect the printed part to detect planar and out of plane error. An example is shown in figure 5. Due to the different reflectivity of the metal powder and the highly reflective printed metal surface, the same intensity parameters of the projected images would cause the overexposure problem as shown in Figure 5. As a result the measured printed surface would loose geometrical information or increase inspection error.



(a) Photograph of printed part (b) Areal map of printed parts

**Figure 5.** Overexposure issue

To correct for this problem the authors have developed a technique to allow for adjustment of projection parameters, as an example a turned manufacturing surface was measured using the system to show inspection ability for lower roughness metal surfaces, as shown in Figure 6.



(a) Photograph of the turning standard sample (b) 3D measurement of the standard sample

**Figure 6.** A turning standard surface measurement result

A set of low quality finished parts manufactured by the AM machine are shown in Figure 7(a). A contact measurement result captured using a Romer Absolute Arm as shown in Figure 7 (b) and is shown in comparison to one of the final in-process layer measurements as shown in figure 7(c). The measurement are not taken in the same location but highlight the capability of the in-process system in detecting geometrical elements of the AM surfaces.

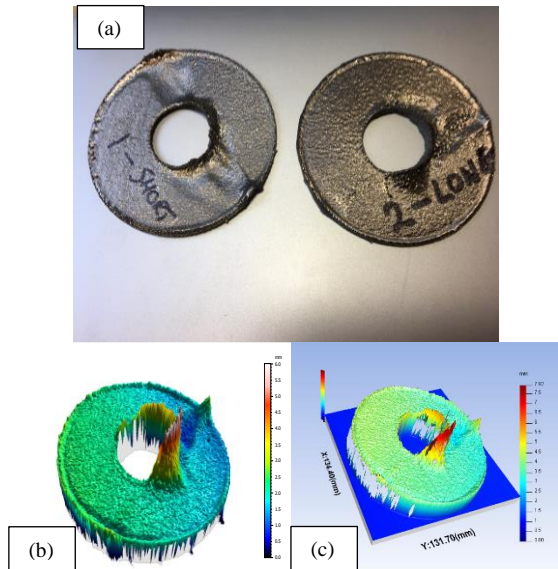


Figure 7. A finished part measurement results

## 5. Conclusions and discussion

In this paper, an in-situ monitoring technique is described in order to facilitate layer wise surface inspection of an EBM AM machine. The measurement system uses a fringe projection technique and shows that areal measurement of the powder bed can insure the accuracy of powder bed before melting and part geometry post melting, this improves process knowledge and facilitates process control. A novel surface fitting algorithm was developed for system calibration and improves measurement accuracy and vertical resolution, this reduced the influence of phase error and random noise. The measurement speed is around 2 secs during each measurement cycle. The presented system is fully integrated into the build cycles of the AM machine providing a “closed door”, high speed measurement process. The system described here is fully adopted for continuous layer by layer measurement, does not require the build environment to be pumped down from vacuum, has a fast acquisition time and has a fully integrated calibration protocol.

There are however several future research directions currently being investigated to improve the system performance and potential application. 1) Automation and intelligent control: employing deep learning algorithms for intelligent measurement, employing pattern recognition techniques to classify defects to realise automation feedback. 2) Combination with other in process inspection techniques to give multi-dimensional data.

## References

- [1] Townsend A, Senin N, Blunt L, Leach RK and Taylor JS 2016 *J. Precision Engineering.* **46** 34-47.
- [2] Schwerdtfeger J, Singer R F, Körner C 2012 *J. Rapid Prototyping J.* **18**(4) 259-263.
- [3] Zhang Z, Towers CE, Towers DP 2006 *J. Opt. Exp.* **14**(14) 6444-55.
- [4] Zhang Z, Huang S, Meng S, Gao F, Jiang X 2013 *J. Opt. Exp.* **21**(10) 12218-27.
- [5] Liu Y, Zhang ZH, Blunt L, Saunby G, Dawes J, Blackham B, et al 2018 *C ASPE and euspen Summer Topical Meeting.* **69** 259-264
- [6] Liu Y, Blunt L, Zhang Z, Rahman H A, Gao F, Jiang X 2020 *J Addit Manuf.* **Vlo 31**, Jan 2020 100940.